MT 26 International Conference on Magnet Technology
Vancouver, Canada | 2019

Tue-Mo-Po2.02-01 [3]

Design of a 70T Quasi-Continuous High Magnetic Field System with a Dual-Coil Magnet

Hongfa Ding, Dake Li, YiLiang Lv, Yun Xu, Liang Li, Peichen Li, Yuchao Fang

Wuhan National High Magnetic Field Center，Huazhong University of Science and Technology, Wuhan, China， 430074

I. Introduction

The quasi-continuous high magnetic field (QCHMF) has been regarded as an acceptable scientific tool in physical, biological and medical fields. Considering the power supply developed at the WHMFC, this paper adopts a hybrid power supply with generator-rectifier power supply (GRPS) and capacitor power supply (CPS) to generate a QCHMF. The parameters of the QCHMF system are obtained via NSGA-II to and a Pareto-scored system to select the results. And a decoupling scheme based on the transformer is adopted to reduce the difficulty of controlling.

II. QCHMF System Design

A. Hybrid Power Supply

GRPS consists of two 12-pulse thyristor rectifiers and a 100 MW/100 MJ pulse generator. The rectifiers are connected in parallel.

CPS is composed of 22 high-density capacitor modules which are charged to 25 kV as an initial voltage.

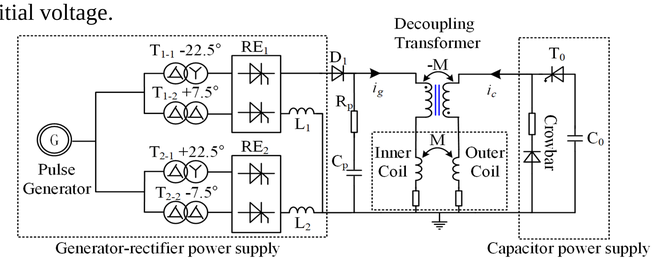

Fig. 1 The fundamental structure of QCMHF system.

B. The mathematical model of the magnet

The magnet field B_0 in the center of coil whose length and thickness is finite and wire is distributed is given by (1). The binary function $F(\alpha, \beta)$ and $G(\alpha, \beta)$ is defined as the magnet field factor and the power factor respectively.

$$\begin{cases} B_0 = Ja_1 \cdot F(\alpha,\beta) \\ F(\alpha,\beta)=\beta \ln \dfrac{\alpha+\sqrt{\alpha^2+\beta^2}}{1+\sqrt{1+\beta^2}} \end{cases} \qquad \begin{cases} B_0 = \sqrt{\dfrac{W}{\rho a_{in}}} \cdot G(\alpha,\beta) \\ G(\alpha,\beta)=\dfrac{1}{5}\beta\sqrt{\dfrac{2\pi\beta}{(\alpha^2-1)}} \cdot \ln \dfrac{\alpha+\sqrt{\alpha^2+\beta^2}}{1+\sqrt{1+\beta^2}} \end{cases} \tag{1}$$

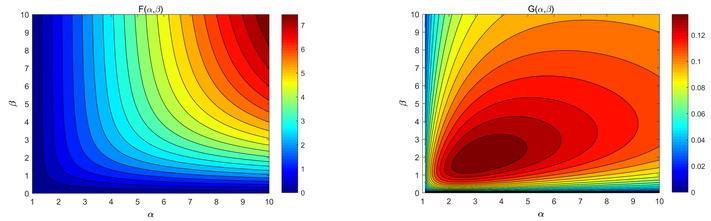

Fig. 2 The contour plot for $F(\alpha, \beta)$ and $G(\alpha, \beta)$.

The joule heat from the energization of power supply will make the resistance and temperature of magnet ascend, which can influence the calculation of electromagnetic and thermal condition. According to the thermal equilibrium, numerical fitting is used to obtain the coupling relation among the circuit, magnet field and joule heat.

$$\begin{cases} x=\int_0^t [J(t)]^2 dt=\int_{T_0}^{T} \dfrac{m}{V}\dfrac{c(T)}{\rho(T)}=F(T)\Big|_{T_0}^{T} \\ T=G(x)=1.9\times10^{-49}x^3-2.887\times10^{-34}x^2+1.601\times10^{-15}x+77 \end{cases} \tag{2}$$

C. Many-objective optimization process

The many-objective optimization of the system design is described as (3).

For an more efficient visualization, the Pareto solutions can be divided into 6 regions via the classification presented in Table I. A scoring system which following the ‘ones vs others’ criteria shown in and Table II is constituted [2].

$$\begin{cases} \vec{X}=(a_{2in}, a_{2out}, h, S_{in}, S_{out}, \lambda_{in}, \lambda_{out}) \\ \vec{y}_i=(F_P, F_D, G_P, G_D, T, I) \\ \text{minimize } \vec{Y}=\left[\vec{y}_1, \vec{y}_2, \cdots, \vec{y}_i\right]=\left[f(\vec{X}_1), f(\vec{X}_2), \cdots, f(\vec{X}_i)\right] \end{cases} \tag{3}$$

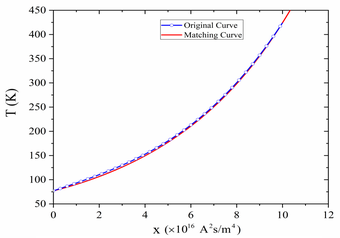

Fig. 3. The curve of $T=G(x)$.

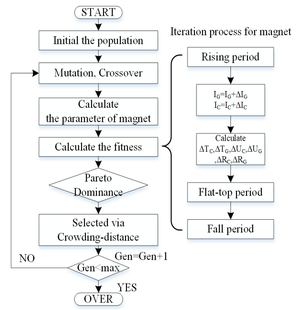

Fig. 4 The flow diagram for NSGA-II [1].

TABLE I Classification of the solutions

	F_P	F_D	G_P	G_D	T_m (K)	I_{Gm} (kA)
HS	(10,+∞)	(0,2)	(0.22,+∞)	(0,0.02)	(0,250)	(0,20)
S	(8,10)	(2,4)	(0.2,0.22)	(0.02,0.04)	(250,280)	(20,21)
T	(6,8)	(4,6)	(0.18,0.20)	(0.04,0.06)	(280,300)	(21,22)
D	(4,6)	(6,8)	(0.16,0.18)	(0.06,0.07)	(300,320)	(22,23)
HD	(2,4)	(8,9)	(0.14,0.16)	(0.07,0.08)	(320,350)	(23,24)
UN	(0,2)	(9,+∞)	(0,0.14)	(0.08,+∞)	(360,+∞)	(24,+∞)

TABLE II Scoring system for Pareto points

Class	Score	Numerical range
HS	k1	[0,1]
S	6×1+1+5×k2	[7,12]
T	6×12+1+10×k3	[73,83]
D	6×83+1+50×k4	[499,549]
HD	6×549+100×k5	[3294,3394]
UN	12306	12306

D. Results of optimization

Based on the process of optimization and scoring system, an appropriate Pareto point with a lower score can be obtained. It can be choose randomly at the Pareto front which has the lowest score.

The selected Pareto points has the objective value of (7.94, 5.98, 0.215, 0.029, 275, 19.7) with the total score (73.54, 82.17, 7.15, 10.21, 10.4, 0.99) is 184.46.

TABLE III Parameters of the Dual-Coil Magnet

	Inner Coil	Outer Coil
Resistance at 77K (mΩ)	14.4	38.6
Inductance (mH)	3.6	40.6
Mutual Inductance (mH)	4.99	
Height (mm)	376	
Outside diameter (mm)	87.1	200.1
Average filling factor	0.48	0.73
Current/Field (A/T)	524.3	530.6
Mass (kg)	43.6	219.2

III. Control Strategy

A. Decoupling scheme

The mutual inductance between the inner coil and outer coil is an obstacle for decreasing the controlling difficulty of the magnetic field, so that a decoupling transformer is an available method.

TABLE III Parameters of the Dual-Coil Magnet

	Inner Coil	Outer Coil
Resistance at 77K (mΩ)	14.4	38.6
Inductance (mH)	3.6	40.6
Mutual Inductance (mH)	-4.99	
Height (mm)	288	
Outside diameter (mm)	76.2	167.8
Mass (kg)	45.8	192.5

B. Self-adaptive PI controller

When the resultant magnet field reaches designed value (70 T), the self-adaptive PI controller starts to adjust the trigger angle of rectifier. In order to promote the control precision, the BP network is used to modifier the proportional coefficient and the integral coefficient [3].

IV. Simulation Clarification

The initial temperature is 77 K. During the period of flat-top pulse, the peak magnetic field of inner coil is 31.7 T with a 19.7 kA current and outer coil is 44.3 T with a 23.2 kA. After the process of energization, the temperature and resistance of inner coil and outer coil changes to 230 K, 106 mΩ and 279 K, 355 mΩ respectively.

The peak von Mises stress in the Zylon reinforce layer is 3.21 GPa which is below the maximum allowable value of 5.8 GPa. The maximum von Mises stress of the Copper-Niobium wire is also quite safe.

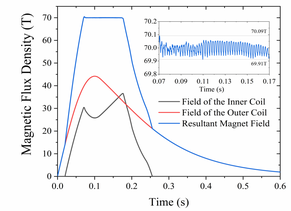

Fig. 5 Magnetic flux density in the center of coil

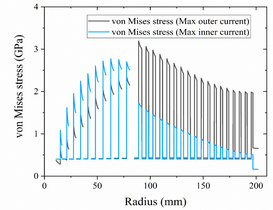

Fig. 6 Distribution of the von Mises stress

V. Conclusion

To summarize, a 70 T/100 ms QCHMF has a ripple less than 1300 ppm with a dual-coil magnet energized by GRPS and CPS is proposed. Based on the mathematical model of the dual-coil magnet, the parameters of the magnet are optimized by the NSGA-II. The decoupling transformer and self-adaptive PI controller is used to improve the stability of the magnetic field. The working conditions of power supply and magnet are gained via co-simulation with MATLAB and COMSOL Multiphysics.

Reference

[1] K. Deb *et al.*, "A fast and elitist multiobjective genetic algorithm: NSGA-II," *IEEE Transactions on Evolutionary Computation*, vol. 6, no. 2, pp. 182-197, 2002.
[2] A. Messac, "Physical programming - Effective optimization for computational design," *AIAA Journal*, vol. 34, no. 1, pp. 149-158, 1996.
[3] H. Ding *et al.*, "Design of a Hybrid Power Supply for a 65 T Quasi-Continuous High Magnetic Field With a Dual-Coil Magnet," *IEEE Transactions on Applied Superconductivity*, vol. 28, no. 3, pp. 1-5, 2018.